Comparing the EM38DD and DUALEM-21S Sensors for Depth-to-Clay Mapping

T. Saey*
D. Simpson
H. Vermeersch
L. Cockx
M. Van Meirvenne
Research Group Soil Spatial Inventory Techniques
Dep. of Soil Management
Faculty of Bioscience Engineering
Ghent Univ.
Coupure 653
B-9000 Gent
Belgium

Geophysical instruments show great potential for the detailed quantification of soil stratigraphy. In this study, two electromagnetic induction sensors were evaluated on their capacity to map small-scale variations of the depth to the interface (z_{in}) in a two-layered soil. On a 2-ha study site, z_{in} between the silty topsoil and the contrasting clayey subsoil was modeled first by relating the two apparent electrical conductivity (EC_a) measurements of the EM38DD sensor to observations of z_{in} obtained by augering. A substantial number of these calibration observations was needed, however, to account for the modeling parameters. To avoid this step, an entirely noninvasive procedure was proposed based on one survey with the DUALEM-21S sensor. This sensor simultaneously records four EC_a values with different coil configurations. These measurements correspond to four different depth response functions that allow modeling z_{in} without calibration observations. The only assumption was a two-layered soil profile. The z_{in} predictions were validated with 24 independent depth observations. Both procedures resulted in equal correlation coefficients (0.85) between predicted and measured z_{in} and average estimation errors (0.26 m). This indicated that both sensors allowed the accurate mapping of the depth to a contrasting textural layer. With the EM38DD, calibration observations are needed, whereas the four different coil conurations of the DUALEM-21S sensor provided sufficient information to predict the interface depth without augering.

Abbreviations: DOE, depth of exploration; EC_a, apparent electrical conductivity; EMI, electromagnetic induction; RMSEE, root mean squared estimation error.

Electromagnetic induction (EMI) is a technique that measures the apparent soil electrical conductivity (EC_a) by inducing an electrical current in the soil. Soil EC_a is controlled by a combination of soil properties, such as porosity, moisture content, concentration of dissolved electrolytes in the soil solution, temperature, and the amount and composition of colloids (McNeill, 1980a). The major advantages of EMI are: (i) it is noninvasive; and (ii) it gives an immediate response. These characteristics have made EMI instruments very popular for the inventory of lateral changes in subsurface soil properties with a fine spatial resolution. In general, EMI is most successful in areas with a single dominant factor of soil variability. Variations in EMI response can be directly related to changes in the dominant property (Doolittle and Collins, 1998).

Previous studies related the EC_a measured with the EM38 sensor (Geonics Ltd., Mississauga, ON, Canada) to the depth and thickness of soil horizons (Doolittle et al., 1994; Bork et al., 1998; Inman et al., 2002; Saey et al., 2008), soil moisture content (Brevik et al., 2006; Huth and Poulton, 2007), clay content (McBratney et al., 2005; Triantafilis and Lesch, 2005), and salinity (Lesch et al., 1998; Amezketa, 2006, 2007). In all of these studies, a single coil spacing was used to derive a relationship between EC_a as measured by the EM38 and the property of interest. With EMI, the depth of investigation is controlled by the coil spacing, coil orientation, frequency of the induced current, and height of the probe above the ground (Gebbers et al., 2007). Because most EMI instruments have a fixed frequency, the only options to control the depth of investigation are coil orientation, coil spacing, and height above the ground. Therefore, colocalized instrument measurements attributed to multiple coil spacings or coil orientations provide more information in depth. Recently, Triantafilis et al. (2003) used the ratio between soil EC_a measurements of EM31 and EM38 instruments, which differ in coil spacing and frequency, to infer a subsurface clay layer underlying sandier sediments in a former stream channel.

With the EM38DD, the soil EC_a is measured simultaneously in two orientations, each having its own depth response profile. The ratio of the two orientations gives an indication of the heterogeneity of the soil profile. This ratio proved to be a useful tool for the delineation of pedologic discontinuities like frost-wedge pseudomorphs (Cockx et al., 2006) and clay lenses (Cockx et al., 2007). Less research has been done to exploit the possibilities of the DUALEM EMI soil sensors (DUALEM, Milton, ON, Canada). These mostly have multiple coil spacings and multiple coil orientations, providing simultaneous measurements with different depth sensitivity. Abdu et al. (2007) compared the EC_a–depth relationship between the DUALEM-1S and Geonics EM38DD sensors. Lee et al. (2006) quantified the effectiveness of the DUALEM-2 in locating a failed septic system in a fine-textured soil.

Soil Sci. Soc. Am. J. 73:7-12
doi:10.2136/sssaj2008.0079
Received 6 Mar. 2008.
*Corresponding author (Timothy.Saey@UGent.be).

Our aim was to accurately characterize the depth to the interface between two contrasting soil layers with the aid of EMI. As a test case, we used a 2-ha study site in central Belgium where Tertiary marine clay was covered by aeolian loess dating from the Weichselian glacial stage. The objective was to compare EC_a measurements obtained with the EM38DD sensor with those of the DUALEM-21S sensor to obtain a continuous, detailed inventory of the field-scale soil stratigraphy.

MATERIALS AND METHODS

Study Site and Geology

The research site was located in Heestert (Belgium), situated in the European loess belt. The site was located on a southeast-facing hillside with an average slope gradient of 7% and an elevation ranging between 30 and 40 m above sea level. The study site was a 2-ha arable parcel (with central coordinates of 50°47′58″ N, 3°24′41″ E). The soil type is an Alfisol according to the U.S. Soil Taxonomy (Soil Survey Staff, 1999) that is characterized by an argillic horizon located between 0.3- to 0.35- and 1.3- to 1.4-m depth.

During the last glacial stage (Weichselian, 80,000–10,000 yr BP), wind-blown loess was deposited over the periglacial undulating landscape of central Europe. In Belgium, this landscape was formed in surfacing Tertiary marine sediments, mostly heavy clay or pure sand, which was exposed to strong erosion during the glacial stages of the Pleistocene. Due to the deposition of the loess, the relief of the Tertiary substrate was smoothed. Depressions were covered by thicker loess than hilltops, and the thickness of the loess was mostly asymmetrical on opposite sides of the hill. As a consequence, the thickness of the loess cover in Belgium varies from a few decimeters to several meters, but rarely exceeds 10 m. Therefore, it is impossible to reconstruct the small-scale differences in depth to the Tertiary substrate based on the present topography (Hubert, 1976). A composite sample taken within the study area showed that the Quaternary loess material consists of 59.0% silt and 13.0% clay, while the Tertiary clayey substrate is composed of 42.4% silt and 54.7% clay.

Electromagnetic Induction Sensors

Two EMI sensors were used: the EM38DD and the DUALEM-21S. The basic operation principle is similar. A transmitter coil located at one end of the instrument generates a primary magnetic field (H_p). This field creates eddy currents in the soil and these time-varying currents induce their own magnetic field (H_i) (McNeill, 1980b). The induced field is superimposed over the primary field and a fraction of both H_p and H_i is intercepted by the receiver coil, where the signal is amplified and formed into an output voltage that is linearly related to EC_a (Rhoades and Corwin, 1981).

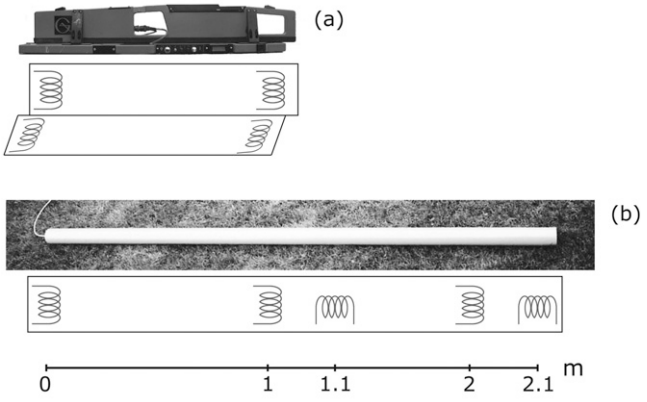

Fig. 1. Transmitter and receiver dipole orientations and coil spacings of the (a) EM38DD and (b) DUALEM-21S.

The EM38DD consists of two EM38 sensors oriented perpendicular to each other. Each EM38 sensor has a transmitter and a receiver coil, 1 m apart. The sensor in the horizontal orientation or dipole mode has both transmitter and receiver coils parallel to the earth's surface while in the vertical dipole mode both coils are perpendicular to the surface (Fig. 1).

The DUALEM-21S sensor consists of a 2.41-m-long tube. This sensor has one transmitter and four receiver coils at different spacings (Fig. 1). The transmitter coil is located at one end, and the receiver coils are at 1-, 1.1-, 2-, and 2.1-m spacing from the transmitter coil. The 1- and 2-m transmitter–receiver pairs form a vertical dipole mode, while the 1.1- and 2.1-m pairs form a perpendicular dipole mode.

So the EM38DD and the DUALEM-21S EMI sensors differ in orientation and distances between the transmitter–receiver coils. Due to the various coil orientations and transmitter–receiver spacings, the DUALEM-21S instrument has a great potential to perform depth soundings.

Both the EM38DD and DUALEM-21S sensors were mounted on a polyethylene sled pulled by an all-terrain vehicle that drove at a speed of 6 to 10 km h^{-1}. Due to the sled construction, the DUALEM-21S instrument was located 0.16 m above the soil surface. The EC_a measurements were recorded at 8 to 10 Hz on a field computer. A Trimble AgGPS332 with Omnistar correction (Trimble Navigation Ltd., Sunnyvale, CA) was used to georeference the EC_a measurements with a pass-to-pass accuracy of approximately 0.10 m. Measurements were taken along parallel lines with an in-between distance of 2 m, and driving was supported by a Trimble Lightbar Guidance System ensuring straight driving lines. Additionally, at each EC_a measurement point, the soil surface elevation was acquired with the Trimble AgGPS332 (accuracy ± 0.30 m). The EC_a measurements were not standardized to a reference soil temperature because both measurements (EM38DD and DUALEM-21S) were performed on the same day, with negligible temperature differences.

Cumulative Depth Response

For the EM38DD and the DUALEM-21S, the cumulative response of a layered medium up to a depth z (m) below the sensor was given by Wait (1962) and McNeill (1980b), for the vertical [$R_v(z)$], horizontal [$R_h(z)$], and perpendicular [$R_p(z)$] modes:

$$R_v(z)=1-\left(4\frac{z^2}{s^2}+1\right)^{-0.5} \quad [1]$$

$$R_h(z)=1-\left(4\frac{z^2}{s^2}+1\right)^{0.5}+2\frac{z}{s} \quad [2]$$

$$R_p(z)=2\frac{z}{s}\left(4\frac{z^2}{s^2}+1\right)^{-0.5} \quad [3]$$

with s being the transmitter–receiver spacing. Based on the different spacings between the DUALEM-21S transmitter and receiver coils, four different cumulative depth response profiles were established.

Figure 2 shows the cumulative response relative to an increase in z of the two coil configurations (vertical [R_v] and horizontal [R_h]) of the EM38DD and the four coil configurations (1-m vertical [$R_{v,1}$],

1.1-m perpendicular [$R_{p,1.1}$], 2-m vertical [$R_{v,2}$], and 2.1-m perpendicular [$R_{p,2.1}$]) of the DUALEM-21S. The general shape of all cumulative sensitivity distributions as found by Callegary et al. (2007) was similar to that predicted by McNeill (1980a). Under electrically conductive conditions, however, lower cumulative responses were observed by Callegary et al. (2007) than McNeill (1980a), especially at deeper depths. Therefore, the models formulated by McNeill (1980a) gave a realistic representation of the depth to the interface at a shallow depth between two soil layers, but with increasing depth there is increasing overestimation.

Due to the quasi-exponential form of the cumulative response curves, the depth of exploration (DOE) can be arbitrarily defined as the depth where 70% of the response is obtained from the soil volume above this depth. This DOE increases for the different coil configurations: $DUALEM_{p,1.1}$, 0.54 m; $EM38_h$, 0.76 m; $DUALEM_{p,2.1}$, 1.03 m; $EM38_v$ or $DUALEM_{v,1}$, 1.55 m; and $DUALEM_{v,2}$, 3.18 m (Fig. 2).

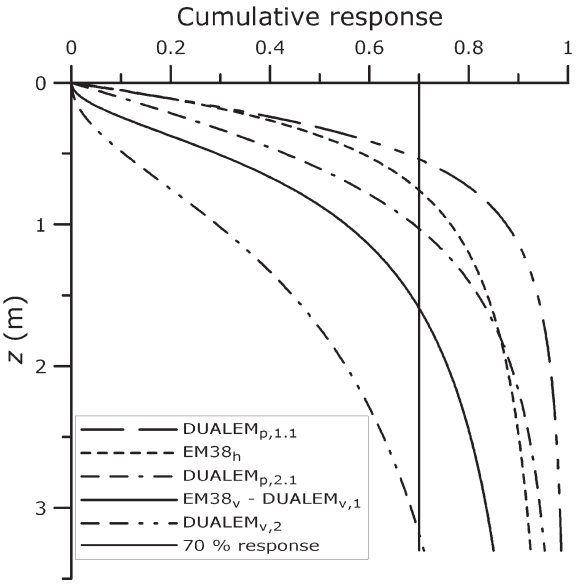

Fig. 2. Cumulative response as a function of the depth *z* for the EM38DD in the horizontal (h) and vertical (v) configurations and the DUALEM-21S in the 1.1- and 2.1-m perpendicular and 1- and 2-m vertical configurations.

RESULTS

Apparent Electrical Conductivity Survey

Table 1 shows the summary statistics of the EM38DD and DUALEM-21S EC_a measurements obtained at the study site. The means of the EC_a values measured with coil configurations that give a larger weight to deeper soil layers are the largest: EC_a-$DUALEM_{v,2}$ ($EC_{av,2}$) > EC_a-$DUALEM_{v,1}$ ($EC_{av,1}$) ~ EC_a-$EM38_v$ (EC_{av}) > EC_a-$DUALEM_{p,2.1}$ ($EC_{ap,2.1}$) > EC_a-$EM38_h$ (EC_{ah}) > EC_a-$DUALEM_{p,1.1}$ ($EC_{ap,1.1}$). The coefficient of variation of these signals was smaller, however. This indicates that in this two-layered soil, the subsoil can be considered more conductive and less heterogeneous than the topsoil.

EM38DD

Ordinary kriging was used to interpolate the EM38DD measurements to a grid of 0.5 by 0.5 m (Goovaerts, 1997). A maximum of 64 neighbors was used within a circular search area with a radius of 20 m around the location being interpolated. The spatial structures of EC_{av} and EC_{ah} were modeled by Gaussian variogram models. The parameters are given in Table 2. The interpolated EC_a maps are shown in Fig. 3a and 3b. Large differences in EC_a were found across short distances, with a similar pattern between EC_{av} and EC_{ah}.

To calibrate EC_{av} and EC_{ah} with the depth to the interface (z_{in}) between the Quaternary silty loess material and clay-rich Tertiary substrate, two calibration transects, ABCD and EF, were laid out. These transects were selected in such a way that both the highest and the lowest EC_a measurements were visited more or less with the same frequency (Fig. 3a). The depth to the interface was measured at 46 observation points along transect ABCD (at 5-m intervals) and 15 points along transect EF (at 3-m intervals). The interface was encountered at 56 observation locations using a gouge auger. At four points of transect ABCD and one point of transect EF, the thickness of the loess exceeded our maximum augering depth of 3.5 m.

The relationship between the EC_a measurements and z_{in} observations was modeled using the McNeill (1980b) cumulative response curves. The main assumptions of this model are a two-layered soil and a uniform EC_a of the Quaternary loess and the Tertiary clayey substrate throughout the field. The cumulative response from the Quaternary topsoil and the Tertiary subsoil can be calculated as $R(z_{in})$ and $1 - R(z_{in})$, respectively, for the vertical and horizontal dipole modes (Eq. [1] and [2]). For each EC_{av} and EC_{ah} measurement, the predicted z_{in} (z_{in}*) can be modeled by solving a system of nonlinear equations. Therefore, the automated function FSOLVE based on the Levenberg–Marquardt algorithm (Marquardt, 1963) in the high-level language and interactive environment Matlab (MathWorks, Natick, MA) was used given the conductivity values of the homogeneous Quaternary topsoil (EC_{aloess}) and the Tertiary clayey subsoil (EC_{aclay}):

$$EC_{av} = [R_v(z_{in}^*)]EC_{aloess} + [1 - R_v(z_{in}^*)]EC_{aclay} \quad [4]$$

$$EC_{ah} = [R_h(z_{in}^*)]EC_{aloess} + [1 - R_h(z_{in}^*)]EC_{aclay} \quad [5]$$

To fit these theoretical relationships to the z_{in}–EC_a data, the sum of the squared differences between z_{in} and z_{in}* was minimized:

$$\sum_{i=1}^{n} [z_{in} - z_{in}^*(i)]^2 = \min \quad [6]$$

Table 1. Descriptive statistics of the apparent electrical conductivity EC_a for the different coil configurations of the electromagnetic induction sensors EM38DD and DUALEM-21S: horizontal (h), vertical (v), 1.1- and 2.1-m perpendicular (p,1.1 and p,2.2), and 1- and 2-m vertical (v,1 and v,2).

Sensor and coil configuration	n	Mean	Min.	Max.	s^2	CV
		mS m^{-1}			(mS m^{-1})^2	%
$EM38_h$	8562	33	6	86	243	47
$EM38_v$	8562	67	29	127	408	30
$DUALEM_{p,1.1}$	10103	29	7	76	175	46
$DUALEM_{p,2.1}$	10103	48	11	110	388	41
$DUALEM_{v,1}$	10103	66	24	124	374	29
$DUALEM_{v,2}$	10103	88	30	136	400	23

Table 2. Variogram parameters of nugget variance (C_0), sill ($C_0 + C_1$), and range (a) of Gaussian variogram models for the variables apparent electrical conductivity in the vertical configuration (EC_{av}), apparent electrical conductivity in the horizontal configuration (EC_{ah}), soil surface elevation (Z), predicted interface depth (z_{in}*) modeled with the EM38DD measurements together with 56 calibration observations, and z_{in}* modeled with the DUALEM-21S measurements.

Measurement	C_0	$C_0 + C_1$	a
			m
EC_{av} (mS m^{-1})	5	225	20
EC_{ah} (mS m^{-1})	5	145	20
Z (m)	0.001	0.601	35
z_{in}* (m), EM38DD + 56 calibration observations	0.005	0.225	20
z_{in}* (m), DUALEM-21S	0.008	0.363	20

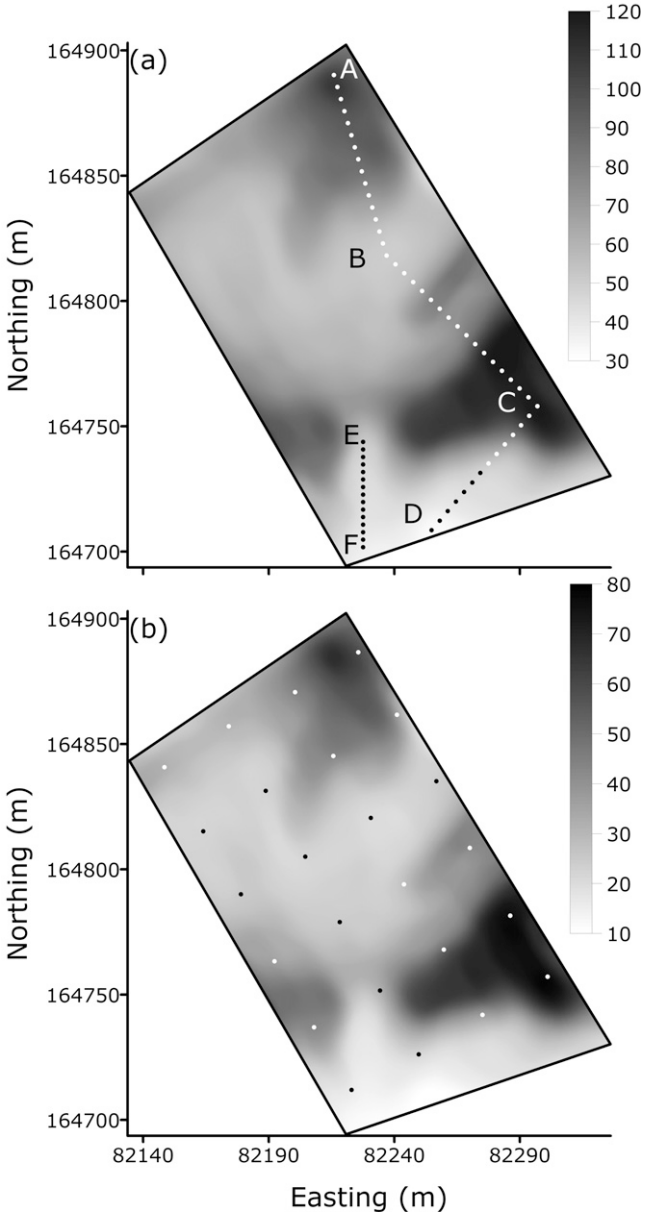

Fig. 3. (a) Interpolated apparent electrical conductivity (EC_a) in the vertical configuration (mS m^{-1}) with localization of calibration points on transects ABCD and EF and (b) EC_a in the horizontal configuration (mS m^{-1}) with localization of validation points.

with n being the number of observations. The parameters EC_{aloess} and EC_{aclay} were iteratively adjusted to obtain the smallest sum of the squared differences between z_{in} and z_{in}*. The obtained values of EC_{aloess} and EC_{aclay} were 12 and 125 mS m^{-1}, respectively. Converted to a reference temperature of 25°C, these values became 15 and 156 mS m^{-1}, respectively, which are similar to the values found by Saey et al. (2008). So, at each measurement point, EC_{av} and EC_{ah} were linked to z_{in}* by using Eq. [1], [2], [4], and [5] as

$$EC_{av} = 12 + \frac{113}{(4 z_{in}{}^{*2} + 1)^{0.5}} \quad [7]$$

$$EC_{ah} = 12 - 226 z_{in}{}^{*} + 113 (4 z_{in}{}^{*2} + 1)^{0.5} \quad [8]$$

This system was solved for z_{in}* with Matlab using the Levenberg–Marquardt algorithm (Marquardt, 1963).

An independent validation was performed to evaluate the predictive quality of this model. Three indices were used as validation criteria: the mean estimation error (MEE), the root mean squared estimation error (RMSEE), and the Pearson correlation coefficient, r. The MEE and RMSEE were obtained from

$$MEE = \frac{1}{n} \sum_{i=1}^{n} [z_{in}{}^{*}(i) - z_{in}(i)] \quad [9]$$

$$RMSEE = \sqrt{\frac{1}{n} \sum_{i=1}^{n} [z_{in}{}^{*}(i) - z_{in}(i)]^2} \quad [10]$$

with n denoting the total number of validation observations. The validation data were obtained as 24 independent observations of the interface depth. These were taken at the centers of 24 grid cells projected over the study site. The observed depths were compared with the model predictions (Fig. 4). A strong correlation between predicted and measured depths (0.85) and a low RMSEE (0.26 m) indicated that this procedure was highly accurate in predicting z_{in}*. On average, however, this procedure overestimated z_{in} with a bias of 0.12 m, as indicated by the MEE.

DUALEM-21S

The four simultaneous EC_a measurements obtained with the quadruple-array DUALEM-21S instrument were used to reconstruct z_{in}. In a two-layered soil, the measured EC_a can be estimated by summing the conductivities and depth-weighted contributions of each layer. Due to the characteristic depth response profiles for each coil configuration, the following four equations could be formulated (taking the height of the DUALEM-21S sensor above the soil surface [0.16 m] into account):

$$EC_{ap,1.1} = \left[R_{p,1.1}(z_{in}{}^{*} + 0.16) - R_{p,1.1}(0.16) \right] EC_{aloess}{}^{*} + \left[1 - R_{p,1.1}(z_{in}{}^{*} + 0.16) \right] EC_{aclay}{}^{*} \quad [11]$$

$$EC_{ap,2.1} = \left[R_{p,2.1}(z_{in}{}^{*} + 0.16) - R_{p,2.1}(0.16) \right] EC_{aloess}{}^{*} + \left[1 - R_{p,2.1}(z_{in}{}^{*} + 0.16) \right] EC_{aclay}{}^{*} \quad [12]$$

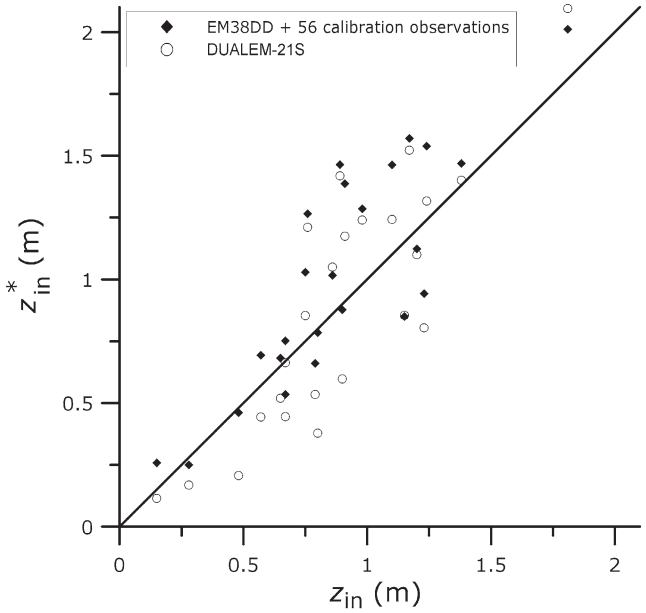

Fig. 4. Scatterplot of predicted interface depth (z_{in}*) vs. the observed depth (z_{in}) for both electromagnetic induction procedures (n = 24).

$$EC_{av,1} = \left[R_{v,1}(z_{in}{*}+0.16) - R_{v,1}(0.16)\right]EC_{aloess}{*} + \left[1 - R_{v,1}(z_{in}{*}+0.16)\right]EC_{aclay}{*} \quad [13]$$

$$EC_{av,2} = \left[R_{v,2}(z_{in}{*}+0.16) - R_{v,2}(0.16)\right]EC_{aloess}{*} + \left[1 - R_{v,2}(z_{in}{*}+0.16)\right]EC_{aclay}{*} \quad [14]$$

with $R_{p,x}(z)$ and $R_{v,x}(z)$ the cumulative responses above a depth z for the perpendicular and vertical dipole modes, respectively, and transmitter–receiver coil spacing of x.

At each measurement location, the nonlinear Eq. [11–14] were combined to model EC_{aloess}*, EC_{aclay}*, and z_{in}*, given the quadruple-array EC_a measurements $EC_{ap,1.1}$, $EC_{ap,2.1}$, $EC_{av,1}$, and $EC_{av,2}$. This system was also solved with Matlab using the Levenberg–Marquardt algorithm.

The summary statistics of EC_{aloess}*, EC_{aclay}*, and z_{in}* within the study site (±10,000 locations) are given in Table 3. The mean EC_{aloess}* is much smaller than the mean EC_{aclay}*, which confirms the subsoil material to be more conductive than the topsoil material. The spatial variability of EC_{aloess}* and EC_{aclay}* reflects a more realistic situation than the assumption of uniformity, which had to be made with the EM38DD. The coefficient of variation indicates that the variability of the top layer is much larger than that of the sublayer. Soil tillage practices might have mixed the Tertiary clayey subsoil with the Quaternary silty topsoil at low interface depths, explaining the larger variability of the topsoil.

The procedure using the DUALEM-21S measurements for predicting z_{in}* was also validated using the same 24 depth observations as in the EM38DD validation. Figure 4 shows the scatterplot of the observed vs. predicted depths. The correlation coefficient between the predicted and measured depths and average error were identical to the values obtained with the EM38DD procedure (r = 0.85 and RMSEE = 0.26 m), with no bias. Therefore, both procedures performed similarly well

Table 3. Descriptive statistics of the predicted apparent electrical conductivity of the topsoil (EC_{aloess}*) and the subsoil (EC_{aclay}*), and the predicted interface depth (z_{in}*) modeled with the DUALEM-21S sensor.

Measurement	Mean	Min.	Max.	s^2	CV
EC_{aloess}*, mS m^{-1}	18	3	31	21	25
EC_{aclay}*, mS m^{-1}	124	85	171	10	3
z_{in}*, m	1.09	0.09	4.90	0.59	70

in estimating z_{in}*. Nevertheless, the DUALEM-21S procedure did not require calibration observations. Moreover, this sensor allowed the estimation of EC_a of the top- and subsoil layers.

Reconstruction of the Interface Depth

Soil surface elevation (Z) and z_{in}* as produced by both sensor procedures were interpolated using ordinary kriging, similarly to the EC_a maps. The variogram parameters are given in Table 2. Figure 5a shows the smooth behavior of the present topography. However, both z_{in}* surfaces, resulting from the two EMI procedures (Fig. 5b and 5c), exhibit a strong small-scale variability of the interface between the Quaternary loess and the Tertiary clay. Moreover, both z_{in}* surfaces show a similar behavior. The DUALEM-21S procedure displays larger detail at greater depths than the EM38DD-based procedure, probably due to the higher DOE of the $DUALEM_{v,2}$ coil configuration.

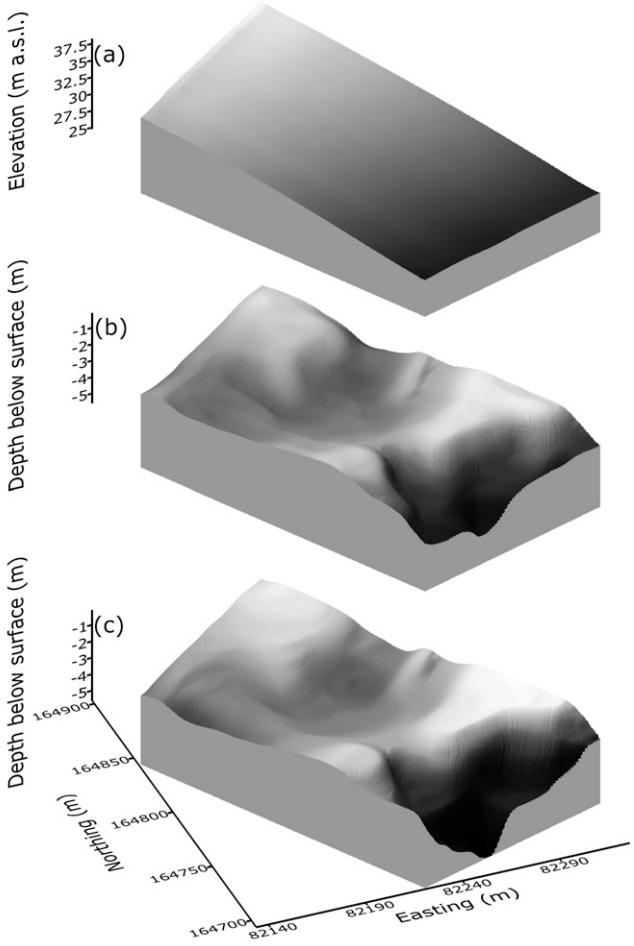

Fig. 5. Elevation of (a) the current soil surface, and the interface depth predicted by (b) the EM38DD procedure and (c) the DUALEM-21S procedure.

CONCLUSIONS

Both EMI sensors allowed accurate prediction of z_{in} in a two-layered soil in a rapid, effective, and nondestructive manner. With the EM38DD, a number of soil auger observations is required to calibrate the EC_a measurements in respect to z_{in}. The quadruple-array DUALEM-21S instrument avoids the need for calibration augering. Its rich information enables a quantification of z_{in} with a similar predictive accuracy. Additionally, it provides inventories of the spatial variability in top- and subsoil conductivity.

ACKNOWLEDGMENTS

This research was supported by the Fund for Scientific Research-Flanders (FWO-Vlaanderen). We thank Mr. M. Coussement for granting access to his field.

REFERENCES

Abdu, H., D.A. Robinson, and S.B. Jones. 2007. Comparing bulk soil electrical conductivity determination using the DUALEM-1S and EM38-DD electromagnetic induction instruments. Soil Sci. Soc. Am. J. 71:189–196.

Amezketa, E. 2006. An integrated methodology for assessing soil salinization, a pre-condition for land desertification. J. Arid Environ. 67:594–606.

Amezketa, E. 2007. Use of an electromagnetic technique to determine sodicity in saline-sodic soils. Soil Use Manage. 23:278–285.

Bork, E.W., N.E. West, J.A. Doolittle, and J.L. Boettinger. 1998. Soil depth assessment of sagebrush grazing treatments using electromagnetic induction. J. Range Manage. 51:469–474.

Brevik, E.C., T.E. Fenton, and A. Lazari. 2006. Soil electrical conductivity as a function of soil water content and implications for soil mapping. Precis. Agric. 7:393–404.

Callegary, J.B., T.P.A. Ferré, and R.W. Groom. 2007. Vertical spatial sensitivity and exploration depth of low-induction-number electromagnetic-induction instruments. Vadose Zone J. 6:158–167.

Cockx, L., G. Ghysels, M. Van Meirvenne, and I. Heyse. 2006. Prospecting frost-wedge pseudomorphs and their polygonal network using the electromagnetic induction sensor EM38DD. Permafrost Periglacial Processes 17:163–168.

Cockx, L., M. Van Meirvenne, and B. De Vos. 2007. Using the EM38DD soil sensor to delineate clay lenses in a sandy forest soil. Soil Sci. Soc. Am. J. 71:1314–1322.

Doolittle, J.A., and M.E. Collins. 1998. A comparison of EM induction and GPR methods in areas of karst. Geoderma 85:83–102.

Doolittle, J.A., K.A. Sudduth, N.R. Kitchen, and S.J. Indorante. 1994. Estimating depth to clays using electromagnetic induction methods. J. Soil Water Conserv. 49:572–575.

Gebbers, R., E. Lück, and K. Heil. 2007. Depth sounding with the EM38-detection of soil layering by inversion of apparent electrical conductivity measurements. p. 95–102. *In* J.V. Stafford (ed.) Precision Agriculture '07. Wageningen Acad. Publ., Wageningen, the Netherlands.

Goovaerts, P. 1997. Geostatistics for natural resources evaluation. Oxford Univ. Press, New York.

Hubert, P. 1976. Verklarende tekst bij het kaartblad: Zwevegem 97E. Hoste-Staelens, Gent.

Huth, N.I., and P.L. Poulton. 2007. An electromagnetic induction method for monitoring variation in soil moisture in agroforestry systems. Aust. J. Soil Res. 45:63–72.

Inman, D.J., R.S. Freeland, J.T. Ammons, and R.E. Yoder. 2002. Soil investigations using electromagnetic induction and ground-penetrating radar in southwest Tennessee. Soil Sci. Soc. Am. J. 66:206–211.

Lee, B.D., B.J. Jenkinson, J.A. Doolittle, R.S. Taylor, and J.W. Tuttle. 2006. Electrical conductivity of a failed septic system soil absorption field. Vadose Zone J. 5:757–763.

Lesch, S.M., J. Herrero, and J.D. Rhoades. 1998. Monitoring for temporal changes in soil salinity using electromagnetic induction techniques. Soil Sci. Soc. Am. J. 62:232–242.

Marquardt, D. 1963. An algorithm for least-squares estimation of nonlinear parameters. SIAM J. Appl. Math. 11:431–441.

McBratney, A., B. Minasny, and B.M. Whelan. 2005. Obtaining 'useful' high-resolution soil data from proximally-sensed electrical conductivity/resistivity (PSEC/R) surveys. p. 503–510. *In* J.V. Stafford (ed.) Precision agriculture '05. Wageningen Acad. Publ., Wageningen, the Netherlands.

McNeill, J.D. 1980a. Electrical conductivity of soils and rocks. Tech. Note TN-5. Geonics Ltd,, Mississauga, ON, Canada.

McNeill, J.D. 1980b. Electromagnetic terrain conductivity measurement at low induction numbers. Tech. Note TN-6. Geonics Ltd,, Mississauga, ON, Canada.

Rhoades, J.D., and D.L. Corwin. 1981. Determining soil electrical conductivity–depth relations using an inductive electromagnetic soil conductivity meter. Soil Sci. Soc. Am. J. 45:255–260.

Saey, T., D. Simpson, U. Vitharana, H. Vermeersch, J. Vermang, and M. Van Meirvenne. 2008. Reconstructing the paleotopography beneath the loess cover with the aid of an electromagnetic induction sensor. Catena 74:58–64.

Soil Survey Staff. 1999. Soil Taxonomy: A basic system of soil classification for making and interpreting soil surveys. 2nd ed. U.S. Gov. Print. Office, Washington, DC.

Triantafilis, J., I.A. Huckel, and I.O.A. Odeh. 2003. Field-scale assessment of deep drainage risk. Irrig. Sci. 21:183–192.

Triantafilis, J., and S.M. Lesch. 2005. Mapping clay content variation using electromagnetic induction techniques. Comput. Electron. Agric. 46:203–237.

Wait, J.R. 1962. A note on the electromagnetic response of a stratified earth. Geophysics 27:382–385.